CRYSTAL GROWTH & DESIGN

Article

pubs.acs.org/crystal

Crystal Engineering Approach toward Selective Formation of an Asymmetric Supramolecular Synthon in Primary Ammonium Monocarboxylate (PAM) Salts and Their Gelation Studies

Tapas Kumar Adalder and Parthasarathi Dastidar*

Department of Organic Chemistry, Indian Association for the Cultivation of Science, 2A & 2B Raja S. C. Mullick Road, Jadavpur, Kolkata 700032, West Bengal, India

Supporting Information

ABSTRACT: A crystal engineering approach assisted by Cambridge Structural Database (CSD) analyses was adopted in synthesizing a new series of primary ammonium monocarboxylate (PAM) salts derived from variously substituted phenylacetic acid (**PA**) and chiral amines (*R*)- and (*S*)-1-phenylethyl amines (**PEA**) with the aim of ascertaining an asymmetric one-dimensional (1D) PAM synthon (designated as synthon W) over the other symmetric possibility (synthon X). Characterization of 32 such PAM salts by single crystal X-ray diffraction (SXRD) revealed the exclusive formation of synthon W. The results suggested that the chiral ammonium components must have played a crucial role in generating exclusive formation of synthon W. Interestingly, about 28% of the PAM salts thus synthesized herein displayed gelation ability thereby emphasizing the role of 1D PAM synthon W in gelation.

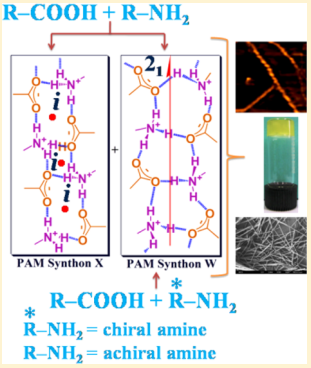

INTRODUCTION

Supramolecular gel, a solid-like material containing mostly solvent and a small amount of solute (gelator—also known as low molecular weight gelators or LMWGs[1]), has gained widespread appeal ranging from academic interests to technological applications.[2] However, the mechanistic interpretation[3] of the gelation process is poorly understood. Studies indicate that the gelator molecules self-assemble to form fibrils driven by various noncovalent interactions such as hydrogen bonding,[4] halogen bonding,[5] $\pi-\pi$ stacking,[6] hydrophobic interactions,[7] charge transfer,[8] etc. The fibrils then self-assemble to form a network structure known as self-assembled fibrillar networks (SAFINs).[9] Immobilization of gelling solvent within SAFINs via capillary forces ultimately results in gel. Macroscopic visualization of such an event is evident from the ability of a gel sample to withstand its own weight against gravity. Unfortunately, molecular level understanding of the gel-forming mechanism is in its infancy, and therefore designing a gelator molecule is indeed a daunting challenge. Nevertheless, efforts have been made by various groups to design gelators.[10]

We have been engaged in designing salt-based organic gelators following a supramolecular synthon[11] approach in the context of crystal engineering[12] and have identified various gel-forming supramolecular synthons, namely, primary ammonium monocarboboxylate (PAM),[13] primary ammonium dicarboxylate (PAD),[14] secondary ammonium monocarboxylate (SAM),[15] and secondary ammonium dicarboxylate (SAD).[16] Among these synthons, the PAM synthon is quite intriguing, and there are mainly two kinds of PAM synthons—both a one-dimensional (1D) columnar hydrogen bonded network (HBN) containing 10-membered (asymmetric synthon W) and alternating 8- and 12-membered (symmetric synthon X) hydrogen bonded rings (Scheme 1). Occasionally, different kinds of two-dimensional (2D) HBNs are also observed in PAM salts.

The crystal structures of 34 PAM salts reported by us thus far revealed that the number of PAM synthons W and X, and other PAM synthons were 16, 14 and 4, respectively. Interestingly 13 out of 16 PAM salts containing PAM synthon W were gelators, whereas only 3 out of 14 PAM salts containing PAM synthon X exhibited gelation, which clearly indicated the effective role of the PAM synthon W in gelation. Understandably, gaining control over the exclusive formation of the PAM synthon W appears attractive in the context of crystal engineering and designing new gelators.

Thus, 32 PAM salts derived from variously substituted phenylacetic acid (**PA**) and both (*R*)- and (*S*)-1-phenylethyl amines (**PEA**) were synthesized (Scheme 2). Single crystal structures of all the PAM salts revealed the exclusive formation of synthon W. This article reports the rationale behind achieving such remarkable control over the formation of synthon W and its role in gelation in this new series of PAM salts.

Received: December 14, 2013
Revised: April 1, 2014
Published: April 1, 2014

dx.doi.org/10.1021/cg401863s | *Cryst. Growth Des.* 2014, 14, 2254−2262

Scheme 1. Most Frequently Observed PAM Synthons "W" and "X"

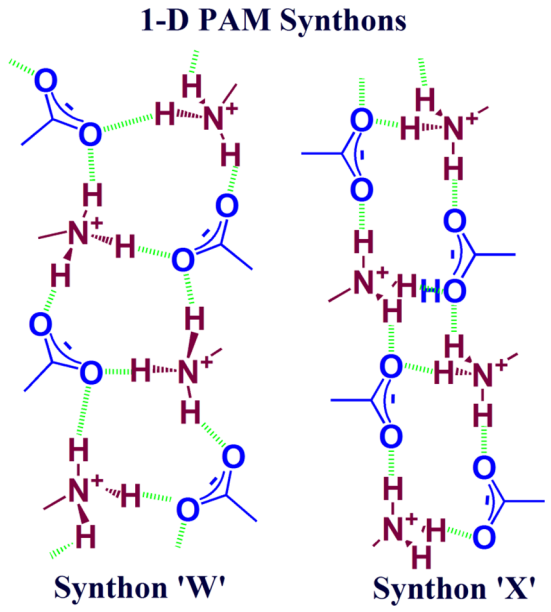

RESULTS AND DISCUSSION

CSD Analyses. To achieve such a goal, we first looked into the Cambridge Structural Database (CSD version 1.15) for PAM salts with $-COO^-$ and NH_3^+ as a search fragment. The number of hits obtained was 2685. Excluding solvate and other functionality capable of forming hydrogen bond resulted in 224 hits, which were then divided into four categories wherein all the possible combinations of aromatic and aliphatic moieties of both the cation and anion of the salts were considered. PAM synthon W was found to be dominating in categories II and IV (~66 and ~56%, respectively); categories I and III were not considered due to an insignificant number of hits (Scheme 3). A close look at the PAM synthon W revealed that there were three kinds of hydrogen bonds involving the ammonium cation and the carboxylate anion leading to the formation of a 1D columnar network propagating along a chiral 2-fold screw axis (2_1-screw). On the other hand, synthon X was intrinsically centrosymmetric having a center of inversion relating alternating 8- and 12-membered hydrogen bonded rings. In fact, further analyses suggested that chirality of the reacting components indeed had an influence on the formation of PAM synthon W; thus, ~48% of the PAM salts in category II having synthon W had chiral amines, whereas nearly 67% of the PAM salts containing synthon W in category IV contained chiral amines. Moreover, a detailed study of PAM salts derived from chiral amines and achiral acids indicated that the chirality of the amine indeed played a crucial role in shaping up the resultant supramolecular synthon;[17] it was observed that ~72% of the salts studied in these reports displayed PAM synthon W. In a series of systematic studies pertaining to the supramolecular chirality transfer,[18] it was observed that ~79% PAM salts having chiral cationic component displayed synthon W. In a recent report[19] on a series of chiral PAM salts displaying intriguing gelation and slow release of pheromones for certain pests, it was observed that all the salts for which the single crystal structures could be determined showed synthon W. Thus, it was clear that molecular chirality of one of the components of PAM salts played a crucial role in promoting asymmetric PAM synthon W. Moreover, there were reports that suggested chirality played vital role in gelation.[20] Thus, we considered a new series of PAM salts derived from variously substituted phenylacetic acid and a chiral amine, namely, (*R*)- and (*S*)-1-phenylethyl amine for the present study.

Syntheses. All the PAM salts depicted in Scheme 2 were synthesized by reacting the acid and the amine in a 1:1 molar ratio in MeOH at room temperature. After complete evaporation of the solvent, the isolated solids were subjected to Fourier transform infrared spectroscopy (FT-IR). The absence of a band at 1697−1708 cm^{-1} and appearance of a

Scheme 2. 32 PAM Salts Studied in the Present Study

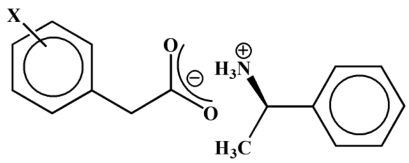

(*R*)-1-phenylethyl amine

X= H;	(*R*)-PEA.PA
2-Br;	(*R*)-PEA.2BPA
3-Br;	(*R*)-PEA.3BPA
4-Br;	(*R*)-PEA.4BPA
2-Cl;	(*R*)-PEA.2CPA
3-Cl;	(*R*)-PEA.3CPA
4-Cl;	(*R*)-PEA.4CPA
2-F;	(*R*)-PEA.2FPA
3-F;	(*R*)-PEA.3FPA
4-F;	(*R*)-PEA.4FPA
2-CH_3;	(*R*)-PEA.2MPA
3-CH_3;	(*R*)-PEA.3MPA
4-CH_3;	(*R*)-PEA.4MPA
2-NO_2;	(*R*)-PEA.2NPA
3-NO_2;	(*R*)-PEA.3NPA
4-NO_2;	(*R*)-PEA.4NPA

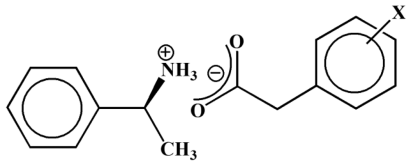

(*S*)-1-phenylethyl amine

X= H;	(*S*)-PEA.PA
2-Br;	(*S*)-PEA.2BPA
3-Br;	(*S*)-PEA.3BPA
4-Br;	(*S*)-PEA.4BPA
2-Cl;	(*S*)-PEA.2CPA
3-Cl;	(*S*)-PEA.3CPA
4-Cl;	(*S*)-PEA.4CPA
2-F;	(*S*)-PEA.2FPA
3-F;	(*S*)-PEA.3FPA
4-F;	(*S*)-PEA.4FPA
2-CH_3;	(*S*)-PEA.2MPA
3-CH_3;	(*S*)-PEA.3MPA
4-CH_3;	(*S*)-PEA.4MPA
2-NO_2;	(*S*)-PEA.2NPA
3-NO_2;	(*S*)-PEA.3NPA
4-NO_2;	(*S*)-PEA.4NPA

dx.doi.org/10.1021/cg401863s | *Cryst. Growth Des.* 2014, 14, 2254−2262

Scheme 3. CSD Search on PAM Salts

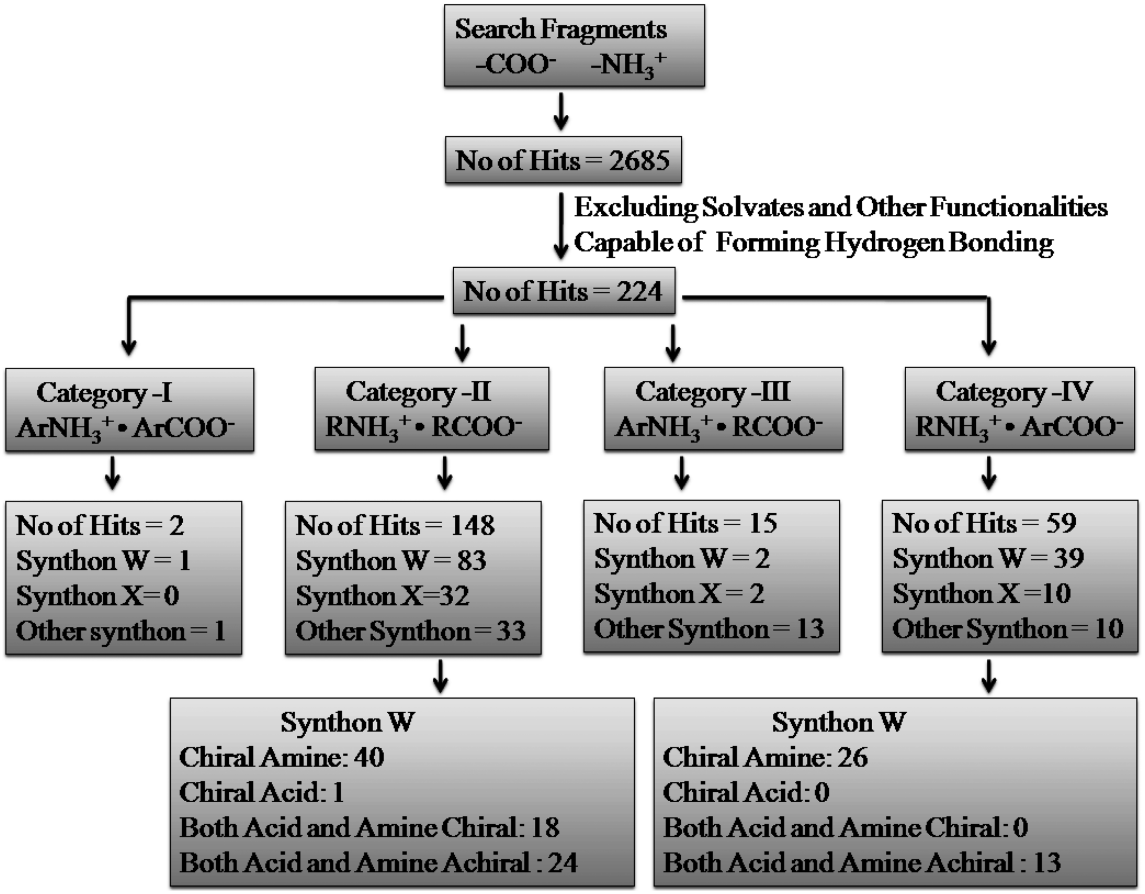

new band at 1533−1587 cm^{-1} clearly indicated that complete deprotonation of the carboxylic acid moiety took place establishing the stoichiometry of these salts as 1:1.

Single Crystal X-ray Diffraction (SXRD). X-ray quality single crystals were obtained from various solvent mixtures (Supporting Information); it may be noted that in each and every crystallization experiment, commercial petrol was needed to get good quality single crystals suitable for X-ray diffraction studies. Fortunately, we were successful in growing single crystals of all 32 salts. SXRD revealed that the salts belonged to three different categories depending on their crystal system and space group (Tables S1−S6, Supporting Information). While most of the salts (17 salts) belonged to the non-centrosymmetric orthorhombic space group $P2_12_12_1$, the rest displayed the non-centrosymmetric monoclinic space groups $P2_1$ (8 salts) and $C2$ (7 salts). Since chirality (*R* or *S*) does not influence the resultant space group (except in the cases of 11 enantiomorphic pairs of space groups), most of the salts having a common carboxylate anion crystallized in the identical space group irrespective of the chirality (R or S) of the ammonium cation; there seems to be, however, an exception for the cases of **(*S*)-PEA·4NPA** ($C2$) and **(*R*)-PEA·4NPA** ($P2_12_12_1$) (entry 13 and 32 respectively, Table 1). On the other hand, the substituents on the phenyl ring of the anionic component appeared to have a significant influence on the resultant space group; thus, unsubstituted or 2-substituted phenyl acetate salts belonged to the space group $P2_1$ (entry 1−8, Table 1), whereas 4-substitution led to the space group $C2$ (entry 9−15, Table 1). All the 3-substituted derivatives crystallized in the space group $P2_12_12_1$ (entry 16−25, Table 1). Interestingly, strongly electron-withdrawing substitution, for example, −F, $-NO_2$ at 2-position led to the space group $P2_12_12_1$ (entry 26−29, Table 1) instead of $P2_1$, whereas an electron-donating substituent, for example, −Me at 4-position displayed $P2_12_12_1$ (entry 30−31, Table 1) instead of $C2$. In each category of the crystals, there were several subgroups containing isomorphous crystal structures; there were 3, 2, and 5 isomorphous subgroups in $P2_1$, $C2$, and $P2_12_12_1$, respectively.

Thus, salts having opposite chirality in the cationic species with identical anionic component or identically positioned substituents in the anionic component (e.g., Me/NO_2 or halogens) were isomorphous except for the salts **(*R*)-PEA·4NPA** ($P2_12_12_1$) and **(*S*)-PEA·4NPA** ($C2$). Detail SXRD analyses of these salts revealed that PAM synthon W was present exclusively in all the crystal structures (Figure 1 and Figures S1−S11, Supporting Information); the carboxylate anion and the ammonium cation were involved in three different kinds of hydrogen bonding sustained by N−H···O interactions [N···O = 2.6822(15)−3.355(3) Å; ∠N−H···O = 145.2−179.4°] that led to the formation of 1D HBN consisting of 10-membered hydrogen bonded rings (synthon W).

It was remarkable that the exclusive formation of PAM synthon W did not depend on the nature of chirality (R or S) of the cationic species, nor did it depend on the position and electronic nature of the substituents on the anionic moiety indicating the robustness of PAM synthon W in this series of salts. In all the cases, the 1D HBN displaying PAM synthon W was packed in parallel fashion along the shortest cell axis *a* or *b*. In most of the cases, the packing of the 1D networks was reinforced by various noncovalent interactions such as C−H···π

dx.doi.org/10.1021/cg401863s | *Cryst. Growth Des.* 2014, 14, 2254−2262

Table 1. Various Crystallographic Parameter and Gelation Property of the Salts

entry	salt	space group	cell parameters (a, b, c, β)	synthon	G/NG[a]
2	(*R*)-PEA·PA	$P2_1$	15.748(9), 6.067(3), 15.816(8), 104.771(16)	W	G
1	(*S*)-PEA·PA	$P2_1$	15.748(9), 6.067(3), 15.816(8), 104.771(16)	W	G
3	(*R*)-PEA·2BPA	$P2_1$	9.1696(3), 6.1000(2), 14.0886(6), 102.164(2)	W	NG
4	(*S*)-PEA·2BPA	$P2_1$	9.0497(4), 6.0462(3), 13.8277(6), 100.174(2)	W	NG
5	(*R*)-PEA·2CPA	$P2_1$	9.1044(4), 6.1014(3), 14.0785(6), 102.4640(10)	W	NG
6	(*S*)-PEA·2CPA	$P2_1$	8.9899(4), 6.0200(3), 13.8303(6), 100.963(3)	W	NG
7	(*R*)-PEA·2MPA	$P2_1$	11.6182(10), 6.0241(5), 11.6695(10), 106.132(2)	W	NG
8	(*S*)-PEA·2MPA	$P2_1$	11.6215(10), 6.0357(5), 11.6740(10), 106.130(2)	W	NG
9	(*R*)-PEA·4BPA	$C2$	18.814(4), 5.7401(12), 14.803(3), 91.957(5)	W	NG
10	(*S*)-PEA·4BPA	$C2$	18.7783(9), 5.7284(3), 14.7747(6), 91.946(5)	W	NG
11	(*R*)-PEA·4CPA	$C2$	18.7305(10), 5.7286(3), 14.6009(8), 91.488(3)	W	NG
12	(*S*)-PEA·4CPA	$C2$	18.2329(6), 5.6931(2), 14.5435(4), 92.2190(10)	W	NG
13	(*S*)-PEA·4NPA	$C2$	18.4839(6), 5.86480(10), 14.7362(4), 94.277(3)	W	G
14	(*R*)-PEA·4FPA	$C2$	20.1479(17), 6.3269(5), 12.3797(10), 92.249(5)	W	NG
15	(*S*)-PEA·4FPA	$C2$	20.1528(9), 6.3263(3), 12.3730(5), 92.303(4)	W	G
16	(*R*)-PEA·3BPA	$P2_12_12_1$	6.4736 (16), 12.144(3), 20.562(5),	W	NG
17	(*S*)-PEA·3BPA	$P2_12_12_1$	6.4741(3), 12.1369(5), 20.5318(8)	W	NG
18	(*R*)-PEA·3CPA	$P2_12_12_1$	6.4880(3), 12.0928(6), 20.1117(10)	W	NG
19	(*S*)-PEA·3CPA	$P2_12_12_1$	6.4865(7), 11.9271(12), 19.820(2)	W	NG
20	(*R*)-PEA·3FPA	$P2_12_12_1$	6.4720(5), 12.2437(8), 19.4058(14)	W	G
21	(*S*)-PEA·3FPA	$P2_12_12_1$	6.5083(2), 12.0454(3), 18.8508(5)	W	G
22	(*R*)-PEA·3MPA	$P2_12_12_1$	5.7242(3), 12.1610(7), 22.5922(13)	W	NG
23	(*S*)-PEA·3MPA	$P2_12_12_1$	5.7217(3), 12.1561(7), 22.5944(12)	W	NG
24	(*R*)-PEA·3NPA	$P2_12_12_1$	5.7484(5), 12.1833(10), 22.8871(18)	W	G
25	(*S*)-PEA·3NPA	$P2_12_12_1$	5.7438(3), 12.1764(7), 22.8889(12)	W	G
26	(*R*)-PEA·2FPA	$P2_12_12_1$	5.9075(11), 12.565(2), 20.215(4)	W	NG
27	(*S*)-PEA·2FPA	$P2_12_12_1$	5.9102(7), 12.5547(15), 20.197(2)	W	NG
28	(*R*)-PEA·2NPA	$P2_12_12_1$	6.8857(5), 12.8536(9), 18.8943(14)	W	NG
29	(*S*)-PEA·2NPA	$P2_12_12_1$	6.873(4), 12.792(6), 18.270(9)	W	NG
30	(*R*)-PEA·4MPA	$P2_12_12_1$	6.7277(8), 8.5988(10), 27.314(3)	W	NG
31	(*S*)-PEA·4MPA	$P2_12_12_1$	6.7196(11), 8.5932(14), 27.330(5)	W	NG
32	(*R*)-PEA·4NPA	$P2_12_12_1$	5.7057(8), 15.291(2), 18.545(3)	W	G

[a]G = Gelator and NG = Nongelator.

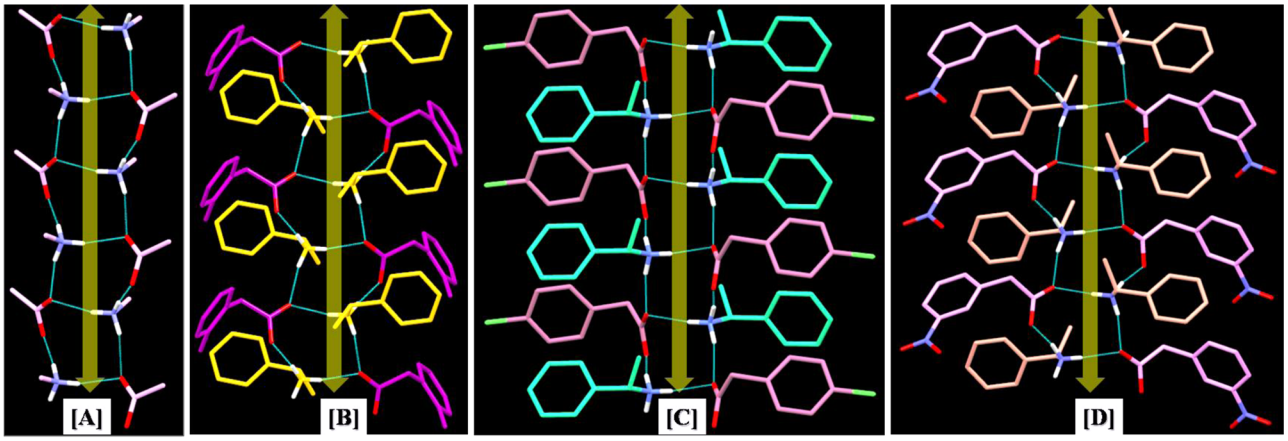

Figure 1. Illustration of single crystal structures; (A) propagation of the 1D HBN displaying PAM synthon W present in all the 32 salts, (B–D) representative examples of PAM synthon W present in the salts (*S*)-**PEA·2MPA**, (*S*)-**PEA·2MPA**, and (*R*)-**PEA·3NPA** belonging to the space group category of $P2_1$, $C2$, and $P2_12_12_1$, respectively.

(3.72–3.76 Å) and C–H···O (3.28–3.78 Å) (Supporting Information). Powder X-ray diffraction (PXRD) confirmed the crystalline phase purity of all the salts except (*R*)- and (*S*)-**PEA·4FPA** (vide infra and Figures S12–S14, Supporting Information).

Gelation Studies. Having established the existence of 1D supramolecular PAM synthon W, we evaluated the gelation ability of these salts by scanning 14 solvents, both polar and nonpolar (Figure 1). The fact that out of 32 salts, only 9 salts (~28%) were found to gel various solvents with good to moderate efficiency displaying minimum gelator concentration (MGC) of 1.8–4.0 wt % with gel–sol dissociation temperature (T_{gel}) of 55–112 °C clearly indicated that the 1D HBN was an important criterion for gelation but not a necessary and

dx.doi.org/10.1021/cg401863s | *Cryst. Growth Des.* 2014, 14, 2254–2262

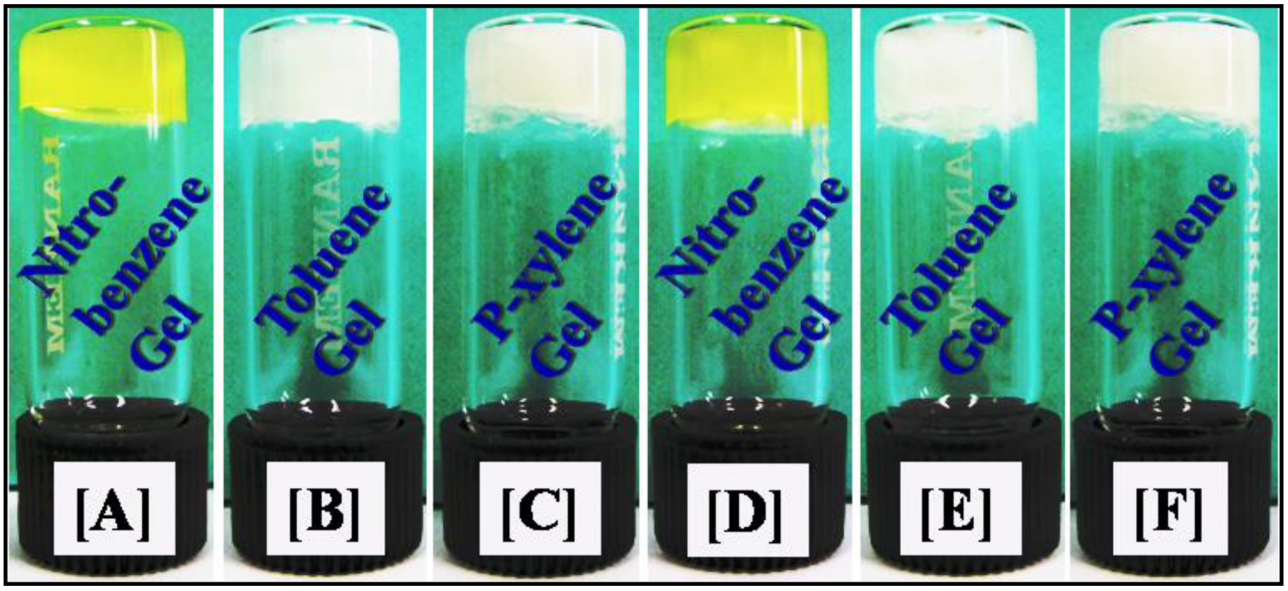

Figure 2. Representative photographs of the 4.0 wt % gel of various gelator salts in different solvents; Panels A–F represent the 4.0 wt % gel derived from (*R*)-**PEA·PA**, (*R*)-**PEA·3NPA**, (*R*)-**PEA·4NPA**, (*S*)-**PEA·PA**, (*S*)-**PEA·3NPA**, and (*S*)-**PEA·4NPA**, respectively.

sufficient condition (Table S7, Supporting Information). Other parameters such as surface compatibility of gel network and target solvent should influence gelation. The position and nature of the substituents on the carboxylate moiety of the PAM salts that might have significant influence on gel network/target solvent interactions seemed to have played a crucial role in gelation. Thus, salts having substituents at 2-position were all nongelators, whereas electron-withdrawing substituents at 3- and 4-positions and also no substitution seemed to have promoted gelation. Salts having an unsubstituted anionic moiety, namely, (*R*)- and (*S*)-**PEA·PA**, were found be the most versatile displaying gelation of 10 solvents out of 14 solvents tested. T_{gel} versus [gelator] plots (Figure 3) of all the 9 gelator salts in various solvents revealed that T_{gel} increased with the increase in gelator concentration in most of the cases indicating the supramolecular nature of the gel network.[21] Because of the lack of common solvent for gelation and differences in MGC, it was not possible to comment on the influence of the substituents on the thermal stability of the gels. However, close inspection of Figure 3 revealed that there were two comparable groups of gelator salts, namely, (*S*)-**PEA·4NPA**, (*R*)-**PEA·3FPA**, (*S*)-**PEA·3NPA** and (*R*)-**PEA·4NPA**, (*S*)-**PEA·PA**, (*R*)-**PEA·3NPA**—both groups gelled a common solvent (*p*-xylene) with different starting gelator concentration (4.0 and 3.0 wt %, respectively); it was observed that 4-NO_2 substituted gelator salts were found to be producing thermally more stable gels than the gels derived from gelator salts having 3-NO_2 substitution in each group displaying the role of the position of the substituents on gelation. It may be mentioned here that all the gels were stable at room temperature for several months.

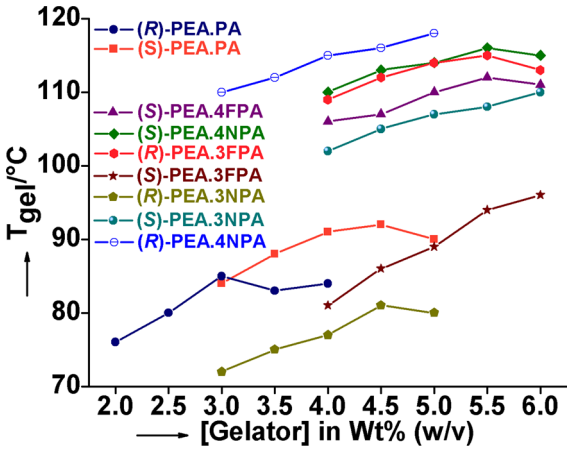

Figure 3. T_{gel} vs [gelator] plots; *p*-xylene [(*S*)-**PEA·PA**, (*S*)-**PEA·3FPA**, (*R*)-**PEA·3NPA**, (*S*)-**PEA·3NPA**, (*R*)-**PEA·4NPA**], mesitylene [(*S*)-**PEA·4NPA**, (*S*)-**PEA·PA**], methyl salicylate [(*R*)-**PEA·3FPA**], and 1,2-dichlorobenzene [(*S*)-**PEA·4FPA**] were employed as gelling solvents.

To assess the viscoelastic response of some of the selected gels, we carried out dynamic rheology wherein the viscous modulus G' and loss modulus G'' were plotted against frequency ω (rad·s^{-1}) with a constant strain of 0.1%. For this purpose, we have chosen an enantiomeric pair of gelators keeping the gelling solvent and concentration of the gelator fixed within the pair. In all the cases studied, G' was significantly more than G'', and they were found to be frequency invariant for a considerable time period thereby establishing their viscoelastic (gel) nature (Figure 4). Critical evaluation of the G' revealed that for the salt **PEA·PA**, the (*S*)-enantiomer was much stronger than (*R*)-enantiomer, whereas the observation was opposite for the salt **PEA·3NPA**. For **PEA·4NPA**, both the enantiomers displayed similar mechanical strength (Table S8, Supporting Information).

Field emission scanning microscopy (FE-SEM) of some selected gels revealed the morphology of the gel network (Figure 5); a bundle of fibers, porous architecture, and highly entangled fibrous networks were observed in the gels. Close inspection of Figure 5C and D revealed the existence of twisted fibers,[22] which was further confirmed by atomic force microscopy (AFM) (Figure 6) on one of the gel (*S*)-**PEA·3NPA** in *m*-xylene); it was clear that most of the fibers observed in the AFM were of left-handed chirality.

dx.doi.org/10.1021/cg401863s | *Cryst. Growth Des.* 2014, 14, 2254–2262

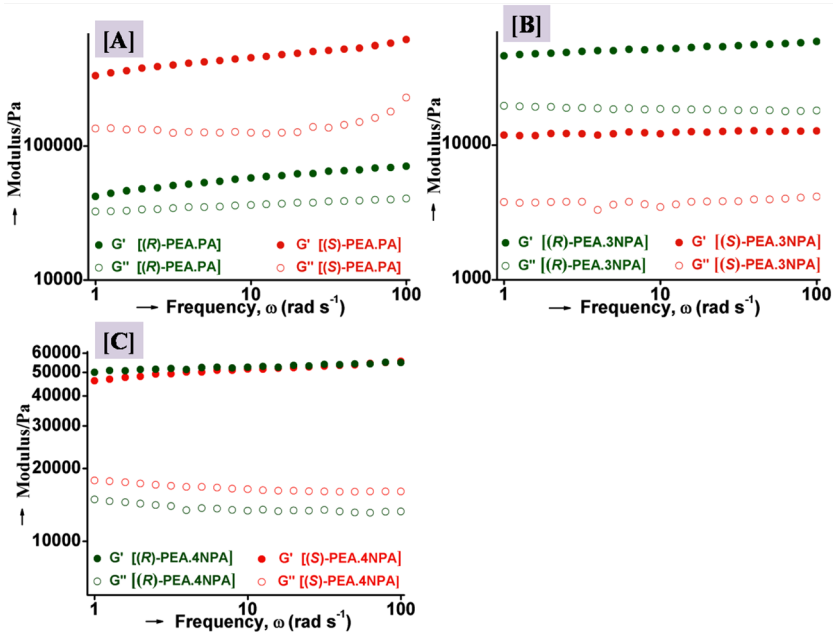

Figure 4. Frequency sweep experiment; (A) 4.0 wt % nitrobenzene gel of (*R*)-**PEA·PA** and (*S*)-**PEA·PA**, (B) 4.0 wt % toluene gel of (*R*)-**PEA·3NPA** and (*S*)-**PEA·3NPA**, (C) 4.0 wt % *p*-xylene gel of (*R*)-**PEA·4NPA** and (*S*)-**PEA·4NPA** at 25 °C.

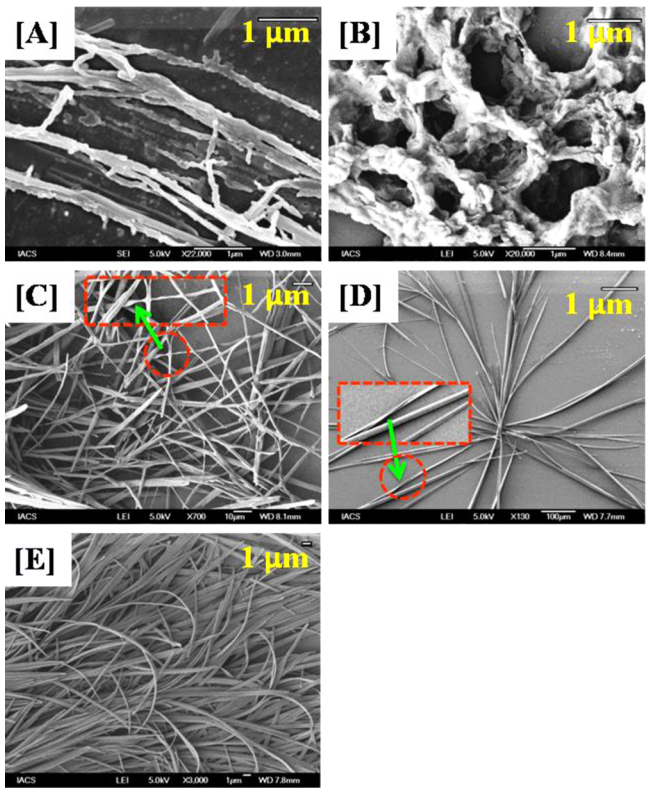

Figure 5. SEM micrographs of the xerogels; (A) (*S*)-**PEA·PA** and (B) (*R*)-**PEA·PA** in mesitylene, (C) (*S*)-**PEA·3NPA** in *m*-xylene, (D) (*S*)-**PEA·3NPA** in toluene, (E) (*S*)-**PEA·3NPA** in *o*-xylene.

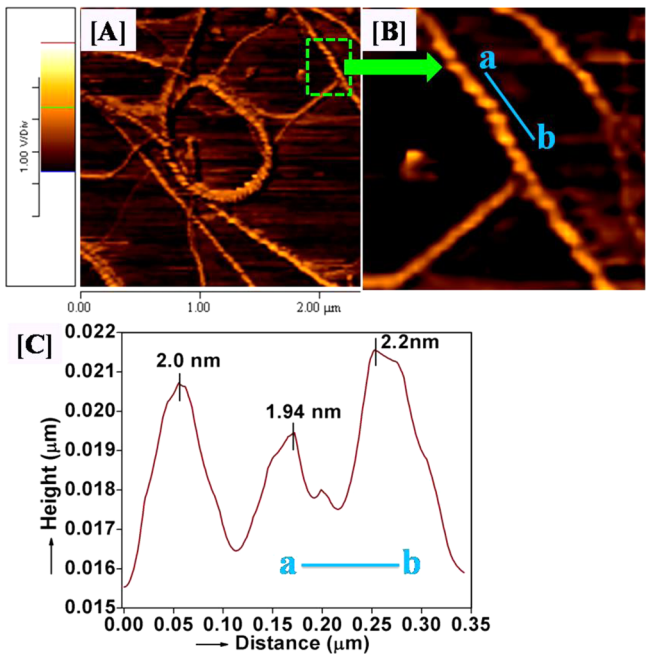

Figure 6. AFM image of the xerogel of (*S*)-**PEA·3NPA** in *m*-xylene. (A) Left-handed helices; (B) zoomed in view of left-handed helices, and (C) height profile of the left-handed helix as marked a–b.

However, a small number of fibers having opposite chirality were also observed. Such an occurrence of a mixture of both left- and right-handed helices from a pure enantiomer was reported to be rare, and it was explained by invoking chiral symmetry-breaking theories.[23] It may be noted here that the chiral amine used for synthesizing these PAM salts was only 98% enantiomerically pure; as a result, the observation of a few fibers having right-handed chirality in AFM could be due to the presence of a small amount of other enantiomers.

Structure–Property Correlation. To probe the role of the supramolecular PAM synthon W on gelation, we attempted structure–property correlation originally proposed by Weiss et al.[24] The PXRD patterns of the xerogels were compared with that of the bulk solid and simulated PXRD patterns obtained from SXRD data. It was revealed that in all the cases, except (*S*)-**PEA·4FPA**, the patterns were nearly superimposable suggesting that the crystal structure determined from SXRD

dx.doi.org/10.1021/cg401863s | *Cryst. Growth Des.* 2014, 14, 2254–2262

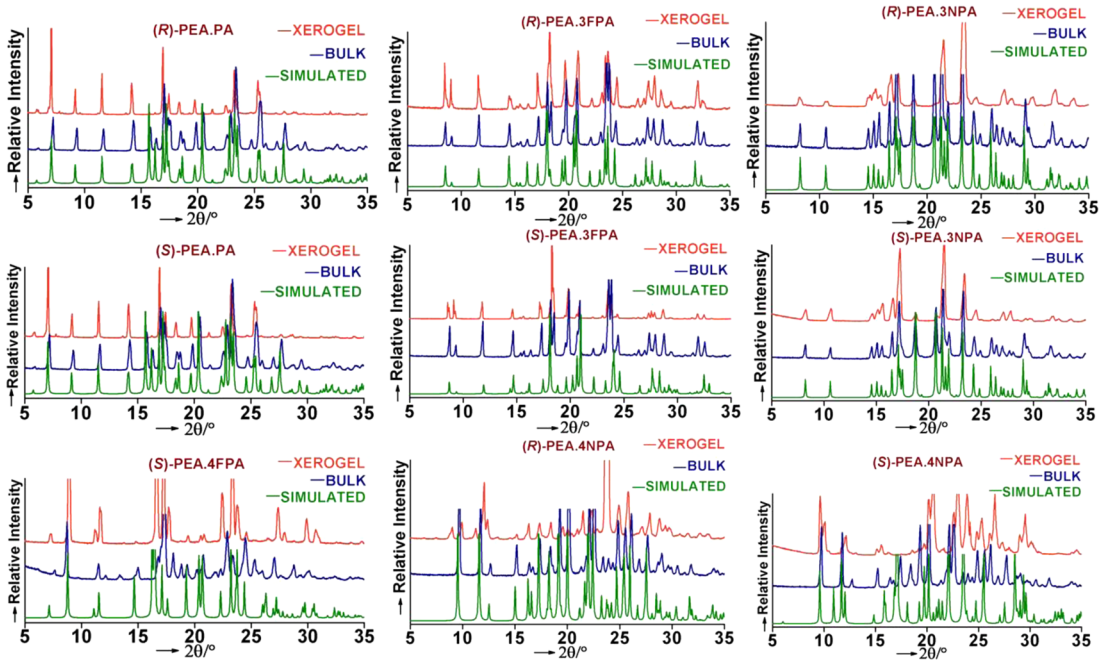

Figure 7. PXRD comparison plots for the gelator salts under various conditions.

truly represented that in the bulk solid as well as in the xerogel (Figure 7). Thus, PAM synthon W was present in these gel networks in the corresponding xerogels. In the case of **(*S*)-PEA·4FPA**, it appeared that PXRD patterns of simulated and xerogel were nearly superimposable, meaning that in this case also synthon W prevailed in the gel network in the xerogel. However, the PXRD pattern of the bulk solid of **(*S*)-PEA·4FPA** showed significant differences from that of the simulated and xerogel PXRDs indicating that there were probably other crystalline phases present in the bulk solid. It may be mentioned that one cannot rule out the possibility of crystalline phase changes or a new event of nucleation resulting in a new crystal phase during xerogel formation due to solvent evaporation. Therefore, ideally PXRD patterns of the gel state should be considered. Acquiring a good quality PXRD pattern from the gel state is often difficult due to the scattering of solvent molecules and less amount of gelators in the gel. However, there is no guarantee that such a phase change should always occur. Thus, comparing PXRD patterns of xerogel in structure−property correlation has been a reasonable compromise.

Conclusions. Control over the exclusive formation of an 1D asymmetric PAM synthon, namely, synthon W, over the other symmetric possibility (synthon X) was achieved in 32 PAM salts by careful consideration of CSD analyses. Introduction of the chiral ammonium cation [(*R*)/(*S*)-1-phenylethylammonium] as one of the components in these PAM salts ensured the exclusive formation of asymmetric PAM synthon W as revealed by SXRD analyses of all the 32 PAM salts. However, only 28% of the PAM salts displayed moderate to good gelation ability with reasonable thermal stability with various polar and nonpolar solvents emphasizing the fact that 1D HBN was an important criterion for gelation but not the necessary and sufficient condition. Position and electronic effects of the substituents seemed to have played important roles in gelation. The position of substituents seemed to have influenced the thermal stability of the gels. Structure−property correlation based on PXRD and SXRD established that the PAM synthon W was present in the xerogel networks as well. Existence of helical fibers in the xerogel of **(*S*)-PEA·3NPA** in *m*-xylene was noteworthy, and a study toward the understanding of expression of molecular chirality into macroscopic chirality (as manifested in twisted fibers) will be undertaken in the future.

EXPERIMENTAL SECTION

Materials and Methods. All the chemicals were commercially available and used as received without further purification. Melting points of all 32 salts were determined by Veego programmable melting point apparatus, India. FT-IR spectra were recorded on a FT-IR-8300, Shimadzu. The elemental compositions of the purified salts were established by elemental analysis (Perkin-Elmer Precisely, Series-II, CHNO/S Analyzer-2400). ^{1}H NMR spectra were recorded on a Brukar AVANCE DPX 300 (for 300 MHz) and III 500 (for 500 MHz). Rheological experiments were performed with an AR 2000 advanced rheometer (TA Instruments). FE-SEM was obtained in a JEOL, JMS-6700F. AFM images were recorded by an AUTOPROBE CP base unit, di CP-II instrument, model no. AP0100. Powder X-ray patterns at various conditions were recorded on a Bruker AXS D8 Advance powder (Cu Kα1 radiation, λ = 1.5406 Å) diffractometer.

General Synthetic Procedure. All 32 salts were synthesized by taking the equimolar amount of the individual components in methanol in a 25 mL beaker. The reaction mixture was sonicated for a few minutes followed by gentle warming if necessary. The resulting solution was kept undisturbed in open air, and a white solid was left after the complete removal of the solvent. The solids were then washed with petroleum ether and recrystallized from either MeOH/petroleum ether or MeOH/commercial petrol. The recrystallized salts were then subjected to various physicochemical analyses and gelation study.

Gelation Study. *T_{gel} Measurements.* In a typical experiment, 20 mg of each salt was taken in a test tube (10 × 100 mm) and dissolved in 500 μL of the targeted solvent by gentle heating. The solution was then allowed to cool to room temperature. Gel formation was confirmed by tube inversion. T_{gel} was measured by the dropping ball method; a glass ball weighing 242.0 mg was placed on top a 0.5 mL gel taken in a test tube. The tube was then immersed in an oil bath placed on a magnetic stirrer to ensure uniform heating. The temperature was noted when the ball touched the bottom of the test tube.

dx.doi.org/10.1021/cg401863s | *Cryst. Growth Des.* 2014, 14, 2254−2262

FE-SEM. Dilute solution of a gelator salt was drop casted on the glass plate fixed with the standard metallic SEM stub and dried under ambient condition. The samples were coated with platinum prior to the SEM image recording.

AFM. The sample for the AFM was prepared by depositing a drop of a dilute *m*-xylene solution of a gelator salt (0.2 wt %) on a cover slide. The sample was dried under a vacuum at room temperature for overnight prior to the recording of AFM images.

Single Crystal X-ray Diffraction. Data were collected using Mo Kα (λ = 0.7107 Å) radiation on a BRUKER APEX II diffractometer equipped with CCD area detector. Data collection, data reduction, structure solution/refinement were carried out using the software package of SMART APEX. All structures were solved by direct method and refined in a routine manner. In most of the cases, non-hydrogen atoms were treated anisotropically. The most of the hydrogen atoms were fixed geometrically. CCDC (CCDC Nos. 953786−953817) contains the supplementary crystallographic data for this paper. These data can be obtained free of charge via www.ccdc.cam.ac.uk/conts/retrieving.html (or from the Cambridge Crystallographic Data Centre, 12 Union Road, Cambridge CB21EZ, UK; fax: (+44) 1223-336-033; or deposit@ccdc.cam.ac.uk).

■ ASSOCIATED CONTENT

Ⓢ Supporting Information

Physicochemical data, gelation data, additional figures, crystallographic parameters, molecular plot with hydrogen bonding parameters, ^{1}H NMR spectra. This material is available free of charge via the Internet at http://pubs.acs.org

■ AUTHOR INFORMATION

Corresponding Author

*E-mail: ocpd@iacs.res.in; parthod123@rediffmail.com.

Notes

The authors declare no competing financial interest.

■ ACKNOWLEDGMENTS

T.K.A. and P.D. thank CSIR, New Delhi, for a senior research fellowship and financial support, respectively. SXRD data were collected at the DBT-funded X-ray diffraction facility under the CEIB program in the Department of Organic Chemistry, IACS, Kolkata.

■ REFERENCES

(1) (a) Weiss, R. G.; Terech, P., Eds. *Molecular Gels: Materials with Self-Assembled Fibrillar Networks*; Springer: Dordrecht, 2005. (b) Fages, F., Eds. Low Molecular Mass Gelators: Design, Self-Assembly, Function. In *Topics in Current Chemistry*; Springer: Dordrecht, 2005; Vol. *256* (Special Issue), pp 1−273. (c) Dastidar, P. *Chem. Soc. Rev.* **2008**, *37*, 2699−2715. (d) Terech, P.; Weiss, R. G. *Chem. Rev.* **1997**, *97*, 3133−3159. (e) Piepenbrock, M.-O. M.; Lloyd, G. O.; Clarke, N.; Steed, J. W. *Chem. Rev.* **2010**, *110*, 1960−2004. (f) Smith, D. K. Molecular Gels - Nanostructured Soft Materials. In *Organic Nanostructures*; Atwood, J. L., Steed, J. W., Eds.; Wiley-VCH: Weinheim, Germany, 2008; pp 111−154. (g) Buerkle, L. E.; Rowan, S. J. *Chem. Soc. Rev.* **2012**, *41*, 6089−6102. (h) Suzuki, M.; Hanabusa, K. *Chem. Soc. Rev.* **2009**, *38*, 967−975. (i) Tsutomu, I.-i.; Shinkai, S. *Top. Curr. Chem.* **2005**, *258*, 119−160. (j) van Esch, J.; Schoonbeek, F.; de Loos, M.; Kooijman, H.; Spek, A. L.; Kellogg, R. M.; Feringa, B. L. *Chem.—Eur. J.* **1999**, *5*, 937−950. (k) Estroff, L. A.; Hamilton, A. D. *Chem. Rev.* **2004**, *104*, 1201−1217. (l) Ajayaghosh, A.; Praveen, V. K.; Vijayakumar, C. *Chem. Soc. Rev.* **2008**, *37*, 109−122.

(2) (a) Hirst, A. R.; Escuder, B.; Miravet, J. F.; Smith, D. K. *Angew. Chem., Int. Ed.* **2008**, *47*, 8002−8018. (b) Kumar, D. K.; Steed, J. W. *Chem. Soc. Rev.* **2014**, *43*, 2080−2088. (c) Sahoo, P.; Sankolli, R.; Lee, H.-Y.; Raghavan, S. R.; Dastidar, P. *Chem.—Eur. J.* **2012**, *18*, 8057−8063. (d) Tam, A. Y.-Y.; Yam, V. W.-W. *Chem. Soc. Rev.* **2013**, *42*, 1540−1567. (e) Li, J.; Kuang, Y.; Gao, Y.; Du, X.; Shi, J.; Xu, B. *J. Am. Chem. Soc.* **2013**, *135*, 542−545. (f) Li, Y.; Rodrigues, J.; Tomás, H. *Chem. Soc. Rev.* **2012**, *41*, 2193−2221. (g) van Bommel, K. J. C.; Friggeri, A.; Shinkai, S. *Angew. Chem., Int. Ed.* **2003**, *42*, 980−999. (h) Liu, Y.; Goebl, J.; Yin, Y. *Chem. Soc. Rev.* **2013**, *42*, 2610−2653. (i) Jung, J. H.; Lee, J. H.; Silverman, J. R.; John, G. *Chem. Soc. Rev.* **2013**, *42*, 924−936. (j) Steed, J. W. *Chem. Soc. Rev.* **2010**, *39*, 3686−3699. (k) Babu, S. S.; Prasanthkumar, S.; Ajayaghosh, A. *Angew. Chem., Int. Ed.* **2012**, *51*, 1766−1776. (l) Díaz, D. D.; Kühbeck, D.; Koopmans, R. J. *Chem. Soc. Rev.* **2011**, *40*, 427−448. (m) Rao, K. V.; Datta, K. K. R.; Eswaramoorthy, M.; George, S. J. *Angew. Chem., Int. Ed.* **2011**, *50*, 1179−1184. (n) Kartha, K. K.; Mukhopadhyay, R. D.; Ajayaghosh, A. *Chimia* **2013**, *67*, 51−63. (o) Carretti, E.; Bonini, M.; Dei, L.; Berrie, B. H.; Angelova, L. V.; Baglioni, P.; Weiss, R. G. *Acc. Chem. Res.* **2010**, *43*, 751−760. (p) Bhagat, D.; Samanta, S. K.; Bhattacharya, S. *Sci. Rep.* **2013**, *3*, 1−8. (q) Tu, T.; Fang, W.; Bao, X.; Li, X.; Dötz, K. H. *Angew. Chem., Int. Ed.* **2011**, *50*, 6601−6605.

(3) (a) Yu, G.; Yan, X.; Han, C.; Huang, F. *Chem. Soc. Rev.* **2013**, *42*, 6697−6722. (b) van Esch, J. H.; Feringa, B. L. *Angew. Chem., Int. Ed.* **2000**, *39*, 2263−2266.

(4) (a) Cantin, K.; Rondeau-Gagné, S.; Néabo, J. R.; Daigle, M.; Morin, J.-F. *Org. Biomol. Chem.* **2011**, *9*, 4440−4443. (b) Rybtchinski, B. *ACS Nano* **2011**, *5*, 6791−6818. (c) Wang, Y.; Zhan, C.; Fu, H.; Li, X.; Sheng, X.; Zhao, Y.; Xiao, D.; Ma, Y.; Ma, J. S.; Yao, J. *Langmuir* **2008**, *24*, 7635−7638.

(5) (a) Meazza, L.; Foster, J. A.; Fucke, K.; Metrangolo, P.; Resnati, G.; Steed, J. W. *Nat. Chem.* **2013**, *5*, 42−47. (b) Priimagi, A.; Cavallo, G.; Metrangolo, P.; Resnati, G. *Acc. Chem. Res.* **2013**, *46*, 2686−2695.

(6) (a) Ajayaghosh, A.; Praveen, V. K. *Acc. Chem. Res.* **2007**, *40*, 644−656. (b) Baddeley, C.; Yan, Z.; King, G.; Woodward, P. M.; Badjić, J. D. *J. Org. Chem.* **2007**, *72*, 7270−7278. (c) Allix, F.; Curcio, P.; Pham, Q. N.; Pickaert, G.; Jamart-Grégoire, B. *Langmuir* **2010**, *26*, 16818−16827. (d) Ryan, D. M.; Doran, T. M.; Nilsson, B. L. *Langmuir* **2011**, *27*, 11145−11156.

(7) (a) Wu, Y.; Wu, S.; Tian, X.; Wang, X.; Wu, W.; Zou, G.; Zhang, Q. *Soft Matter* **2011**, *7*, 716−72. (b) Suzuki, M.; Nakajima, Y.; Yumoto, M.; Kimura, M.; Shirai, H.; Hanabusa, K. *Langmuir* **2003**, *19*, 8622−8624. (c) Tam, A. Y.-Y.; Wong, K. M.-C.; Zhu, N.; Wang, G.; Yam, V. W.-W. *Langmuir* **2009**, *25*, 8685−8695.

(8) (a) Liu, Y.; Yu, Y.; Gao, J.; Wang, Z.; Zhang, X. *Angew. Chem., Int. Ed.* **2010**, *49*, 6576−6579. (b) Haketa, Y.; Sasaki, S.; Ohta, N.; Masunaga, H.; Ogawa, H.; Mizuno, N.; Araoka, F.; Takezoe, H.; Maeda, H. *Angew. Chem., Int. Ed.* **2010**, *49*, 10079−10083.

(9) George, M.; Weiss, R. G. *Acc. Chem. Res.* **2006**, *39*, 489−497.

(10) (a) Maeda, H.; Chigusa, K.; Sakurai, T.; Ohta, K.; Uemura, S.; Seki, S. *Chem.—Eur. J.* **2013**, *19*, 9224−9233. (b) Muro-Small, M. L.; Chen, J.; McNeil, A. J. *Langmuir* **2011**, *27*, 13248−13253. (c) Luboradzki, R.; Gronwald, O.; Ikeda, M.; Shinkai, S.; Reinhoudt, D. N. *Tetrahedron* **2000**, *56*, 9595−9599. (d) van Esch, J.; Schoonbeek, F.; de Loos, M.; Kooijman, H.; Spek, A. L.; Kellogg, R. M.; Feringa, B. L. *Chem.—Eur. J.* **1999**, *5*, 937−950. (e) Samanta, S. K.; Bhattacharya, S. *J. Mater. Chem.* **2012**, *22*, 25277−25287. (f) van Esch, J. *Langmuir* **2009**, *25*, 8392−8394. (g) Chen, J.; Kampf, J. W.; McNeil, A. J. *Langmuir* **2010**, *26*, 13076−13080. (h) Olive, A.G. L.; Raffy, G.; Allouchi, H.; Léger, J.-M.; Guerzo, A.; Desvergne, J.-P. *Langmuir* **2009**, *25*, 8606−8614.

(11) Desiraju, G. R. *Angew. Chem., Int. Ed.* **1995**, *34*, 2311−2327.

(12) (a) Desiraju, G. R.; Vittal, J. J.; Ramanan, A. *Crystal Engineering: A Text Book*; IISc Press and World Scientific: India, 2011. (b) Desiraju, G. R. *Angew. Chem., Int. Ed.* **2007**, *46*, 8342−8356.

(13) Das, U. K.; Banerjee, S.; Dastidar, P. *Chem.—Asian J.* **2013**, *8*, 3022−3031 and references cited therein.

(14) Adalder, T. K.; Kumar, D. P.; Dastidar, P. *Cryst. Growth Des.* **2014**, *14*, 11−14 and references cited therein.

(15) Sahoo, P.; Sankolli, R.; Lee, H.-Y.; Raghavan, S. R.; Dastidar, P. *Chem.—Eur. J.* **2012**, *18*, 8057 and references cited therein.

(16) Sahoo, P.; Dastidar, P. *Cryst. Growth Des.* **2012**, *12*, 5917−5924 and references cited therein.

(17) (a) Kinbara, K.; Hashimoto, Y.; Sukegawa, M.; Nohira, H.; Saigo, K. *J. Am. Chem. Soc.* **1996**, *118*, 3441−3449. (b) Kodama, K.; Kobayashi, Y.; Saigo, K. *Chem.—Eur. J.* **2007**, *13*, 2144−2152.
(18) (a) Nishiguchi, N.; Kinuta, T.; Sato, T.; Nakano, Y.; Tokutome, H.; Tajima, N.; Fujiki, M.; Kuroda, R.; Matsubara, Y.; Imai, Y. *Chem.—Asian J.* **2012**, *7*, 360−366. (b) Nishiguchi, N.; Kinuta, T.; Sato, T.; Nakano, Y.; Harada, T.; Tajima, N.; Fujiki, M.; Kuroda, R.; Matsubara, Y.; Imai, Y. *Cryst. Growth Des.* **2012**, *12*, 1859−1864 and references cited therein.
(19) Sahoo, P.; Kumar, D. K.; Raghavan, S. R.; Dastidar, P. *Chem.—Asian J.* **2011**, *6*, 1038−1047.
(20) (a) Smith, D. K. *Chem. Soc. Rev.* **2009**, *38*, 684−694. (b) Ajayaghosh, A.; Varghese, R.; George, S. J.; Vijayakumar, C. *Angew. Chem., Int. Ed.* **2006**, *45*, 1141−1144. (c) Mateos-Timoneda, M. A.; Crego-Calama, M.; Reinhoudt, D. N. *Chem. Soc. Rev.* **2004**, *33*, 363−372. (d) de Jong, J. J. D.; Lucas, L. N.; Kellogg, R. M.; van Esch, J. H.; Feringa, B. L. *Science* **2004**, *304*, 278−281. (e) Oda, R.; Huc, I.; Schmutz, M.; Candau, S. J.; MacKintosh, F. C. *Nature* **1999**, *399*, 566−569.
(21) Raghavan, S. R.; Cipriano, B. H. *In Molecular Gels. Materials with Self-Assembled Fibrillar Networks*; Weiss, R. G., Terech, P., Eds.; Springer: Dordrecht, 2005; Chapter 8, pp 241−252.
(22) Praveen, V. K.; Babu, S. S.; Vijayakumar, C.; Varghese, R.; Ajayaghosh, A. *Bull. Chem. Soc. Jpn.* **2008**, *81*, 1196−1211.
(23) (a) Thomas, B. N.; Corcoran, R. C.; Cotant, C. L.; Lindemann, C. M.; Kirsch, J. E.; Persichini, P. J. *J. Am. Chem. Soc.* **1998**, *120*, 12178−12186. (b) Thomas, B. N.; Lindemann, C. M.; Corcoran, R. C.; Cotant, C. L.; Kirsch, J. E.; Persichini, P. J. *J. Am. Chem. Soc.* **2002**, *124*, 1227−1233.
(24) Ostuni, E.; Kamaras, P.; Weiss, R. G. *Angew. Chem., Int. Ed.* **1996**, *35*, 1324−1326.